FERMILAB-CONF-17-341-TD 1
ACCEPTED

Measurements of Dynamic Effects in FNAL 11 T Nb_3Sn Dipole Models

G. Velev, T. Strauss, E. Barzi, G. Chlachidze, J. DiMarco, F. Nobrega, I. Novitski, S. Stoynev, D. Turrioni, A.V. Zlobin

***Abstract*—Fermilab, in collaboration with CERN, has developed a double-aperture 11 T Nb_3Sn dipole suitable for the high-luminosity LHC upgrade. During 2012-2014, a 2-m long single-aperture dipole demonstrator and three 1-m long single-aperture dipole models were fabricated by FNAL and tested at its Vertical Magnet Test Facility. Collared coils from two of the 1-m long models were then used to assemble the first double-aperture dipole demonstrator. This magnet had extensive testing in 2015-2016, including quench performance, quench protection, and field quality studies. This paper reports the results of measurements of dynamic effects in the single-aperture and double-aperture 11 T Nb_3Sn dipoles and compares them with similar measurements in previous NbTi magnets.**

***Index Terms*— Accelerator Magnets, Decay and Snap-back, Persistent Currents, Superconducting Magnets.**

I. Introduction

Since the early operation of the Tevatron collider in the late 1980's, control of dynamic effects in superconducting magnets has become an important part of any machine current ramping profile [1]. These effects are especially important during the time of beam injection, when the strong changes of the sextupole field in the main dipoles can generate a significant chromaticity growth. For the Tevatron collider, it was found that this chromaticity change could be up to 70 units during a period of several hours, and as a result, significant beam loss occurred when the current ramped up at the beginning of beam acceleration [1].

As a rule, the most significant changes are observed in the main field and the normal sextupole component of the bending dipoles. For example, the change observed in the normal sextupole component is presented as slow decay from the hysteresis curve during injection dwell. In the next step, when the current is ramped during the beam acceleration, a fast snap-back to the hysteresis curve occurs.

The present understanding of these effects for NbTi magnets is explained in [2]. During the injection dwell, local field changes due to current redistribution decrease, on average, the filament magnetization in the superconducting cable, and consequently affect the allowed harmonic fields in the magnet. Following this model, we do not expect that magnets built with Nb_3Sn superconductor will behave differently. Recently, however, results from the Nb_3Sn 11 T dipole short model program at CERN were published [3], showing discrepancy with this expectation at 1.9 K, which has been well established for NbTi magnets in previous methodical measurements performed for the Tevatron [4, 5, 6], HERA [7], RHIC [8], and LHC [9].

As of today, the magnets for the next generation accelerators (e.g. the High Energy LHC upgrade or the Future Circular Collider) will need Nb_3Sn superconducting magnets to achieve the required nominal operation fields on the level of 15-16 T. During the development of Nb_3Sn magnets over the last 15 years, we have performed a systematic set of measurements on the Nb_3Sn magnets at the Fermilab Vertical Magnet Test Facility (VMTF). These measurements have included dipole models for VLHC [9] and 11 T dipoles for the HL-LHC upgrade [10], as well as quadrupole models and prototypes (demonstrators) for LHC IR upgrade, as part of the US LARP program. Summaries of these measurements are published elsewhere [11].

This paper presents the results from the measurement of the dynamic effects on the Fermilab 11 T short models. Table 1 summarizes the magnets that comprise this study. Three single-aperture modes MBHSP02-04 were measured with a standardized current profile. It includes a high current flat-top, magnet reset at 100 A and injection dwell at 760 A for 30 min, similar to the profile shown in Fig. 1, but without a back

TABLE I
Magnets and Current Profile Parameters

Magnet	I_{inj} (A)	Reset current (A)	Back-porch dwell (min)
MBHSP02	760	100	0
MBHSP03	760	100	0
MBHSP04	760	100	0
MBHDP01*	760	100	0
MBHDP01*	760	0	0
MBHDP01*	760	350	0
MBHDP01*	760	760	0
MBHDP01*	350	100	0
MBHDP01*	1170	100	0
MBHDP01*	1420	100	0
MBHDP01*	350	100	30
MBHDP01*	760	100	30

[a]MBHDP01 is a double-aperture magnet, assembled with the collared coils from MBHSP02 and MBHSP03

Manuscript received August 29, 2017. Work supported by Fermi Research Alliance, LLC, under contract No. DE-AC02-07CH11359 with the U.S. Department of Energy.

The authors are with Fermi National Accelerator Laboratory, P.O. Box 500, Batavia, IL 60510, USA, (e-mail: velev@fnal.gov).

porch. The double-aperture model, MBHDP01, was measured with different variations of the current profile, with parameters as summarized in Table 1.

II. Field Definitions And Measurement System

Typically, the magnetic measurement results are expressed in a standard form of harmonic coefficients defined in a series expansion

$$B_x + iB_y = B_m\, 10^{-4} \sum_{n=1}^{\infty} (b_n + ia_n) \left(\frac{x+iy}{r_0}\right)^{n-1} \qquad (1)$$

where B_x and B_y in (1) are the field components in Cartesian coordinates, b_n and a_n are the 2n-pole normal and skew coefficients at reference radius r_0, normalized by the main field, B_m, and scaled by a factor 10^4 so as to report the harmonics in convenient 'units'. In this paper, all measurements utilize r_0 of 17 mm, which is the nominal value for the LHC dipole magnets.

To measure field components, we use the standard rotating coil technique. The measurement probe is built on circuit board technology [12] and has integration length of 130 mm, which approximately corresponds to one twist pitch of the cable.

The integration component of the data acquisition system is based on ADC and digital signal processor boards [13]. The system can digitize simultaneously 5 channels measuring the magnetic field plus the current signal, tolerating a probe rotation rate of up to 7.5 Hz. For the measurements reported here, to mitigate the noise from the mechanical vibrations of the rotational system, we use a probe speed of 1 Hz.

III. Field Decay

To parameterize the decay in the allowed field components we use the double exponential form as proposed at [6]

$$b_3^{dec} = b_{3,1}\left(1 - \exp\left(-\frac{t}{t_1}\right)\right) + b_{3,2}\left(1 - \exp\left(-\frac{t}{t_2}\right)\right) \qquad (2)$$

Two exponential forms are fitting the fast and slow mode of

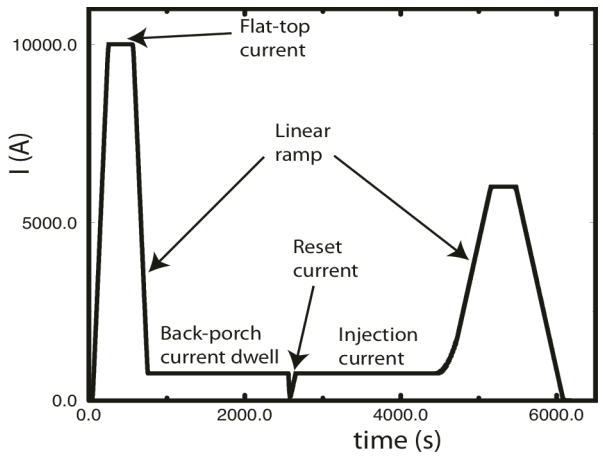

Fig. 1. An example of typical current profile used in the measurements.

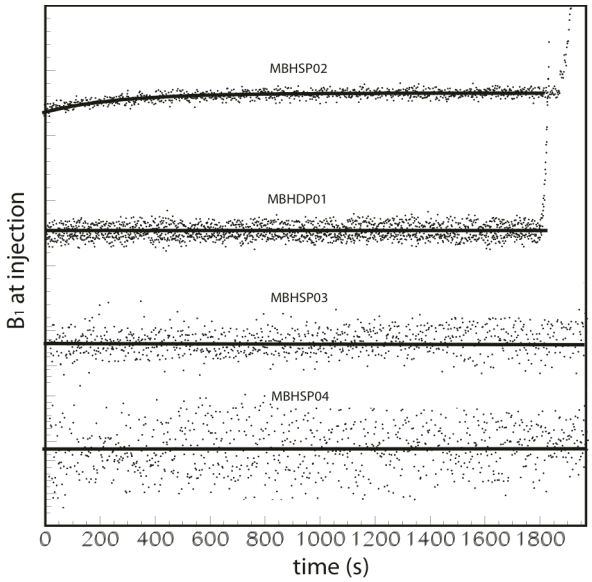

Fig. 2. The main field of the single-aperture models MBHSP02-04 and the double-aperture demonstrator MBHDP01. Only MBHSP02 shows a slight decay of the main field during the injection porch.

the decay, and Eq. 2 is similar to what is used to describe the decay time dependence in the LHC main dipoles [14] and LHC 11 T Nb_3Sn models [3].

As was briefly discussed earlier, the decay can be observed in all allowed harmonics. Fig. 2 shows the dipole field during the injection. In three of the four magnets we did not observe any decay; the fit preferred a constant line. We observed a decay in magnet MBHSP02 best described with a single exponential form with an amplitude of 7.5 10^{-4} T-m (~ 10 units) and a time constant of t_1=255 s.

Typical normal sextupole decay for MBH magnets after 30 min at 760 A injection is shown in Fig. 3. On average, the decay amplitude is at the level of 4 to 7 units, somewhat larger compared to the amplitude observed in NbTi magnets, which is at the level of 1 to 2 units. This could be attributed to larger filaments of the Nb_3Sn in comparison to the NbTi cables.

Table II summarizes the fit results for the b_3 decays with Eq. 2. For the MBHSP02-04 magnets, the fit prefers a single exponential form without a short mode. We found that at 760 A injection (including MBHDP01 along with the

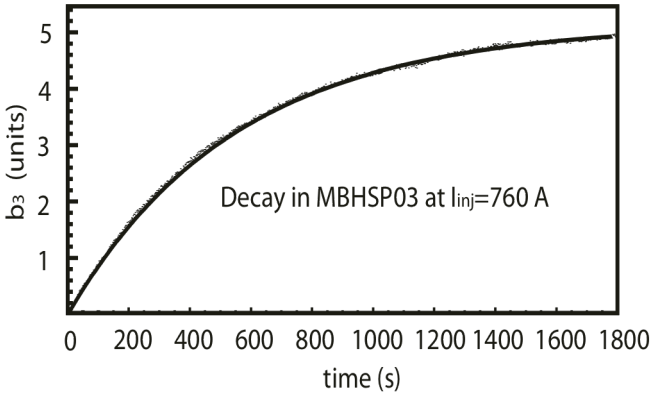

Fig. 3. A typical decay in the MBH dipoles after 30 min dwell at injection (760 A).

TABLE II
DECAY PARAMETERS OBTAINED BY FITTING TO DOUBLE EXPONENTIAL EQ. 2

Magnet	I_{inj} (A)	$b_{3,1}$ (units)	t_1 (s)	$b_{3,2}$ (units)	t_2 (s)	b_3 (units)
MBHSP02	760	6.9	290	0	-	6.9
MBHSP03	760	5.1	302	0	-	5.1
MBHSP04	760	6.5	329	0	-	6.5
MBHDP01	760	2.5	1949	1.0	172	3.5
MBHDP01	350	0.7	630	0.6	32	1.3
MBHDP01	1170	1.7	400	0	-	1.7
MBHDP01	1470	1.6	630	0.3	36	1.8

MDHSP02-04), the average decay amplitude is 5.5 units and the average slow time constant is t_1=718 s.

For the double-aperture model, MBHDP01, we performed several tests varying the injection current. For currents above the full penetration state of the filaments (1170 A and 1470 A), we observed decay amplitudes ($b_{3,1}$, $b_{3,2}$) and time constants (t_1, t_2) comparable to the NbTi magnets reported in [6]. A similar result was obtained for the injection current of 350 A, which is much below the penetration level. Unfortunately, this measurement suffers from large noise due to the sizable flux jumps at lower fields, and this prevents accurate determination of the decay amplitude.

For MBHDP01 we performed a test stopping for 30 min at the upper branch of the hysteresis curve at 760 A. The result is shown in Fig. 4. As expected, the b3 decays inversely, decreasing its value with time. A similar result was reported in [4] but on the lower branch of the hysteresis curve. Moreover, one can see the noise of the measurements due to Nb_3Sn conductor instabilities at this branch of the hysteresis curve.

IV. SNAPBACK MEASUREMENTS

To compare the measurements with different parameters of the current cycle and different magnets, first we must remove the effect of the hysteresis curve underlying the snapback. We empirically estimate the behavior of this curve directly using the b_3 cycle measurements and performing a parabolic fit of the points in the adjacent regions before and after the snapback. In several papers [6, 9], it was found that parabolic fit

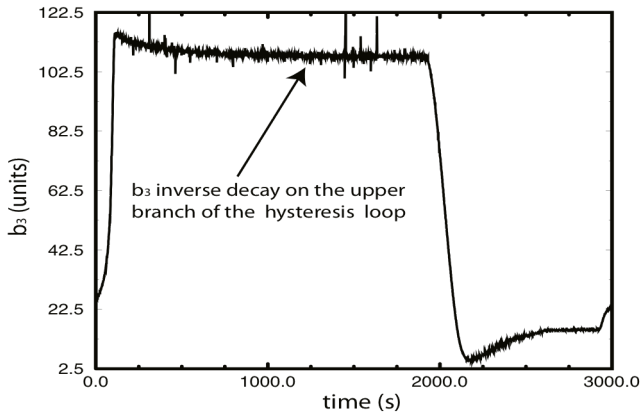

Fig. 4. An example of inverse decay of the upper branch of the sextupole hysteresis loop.

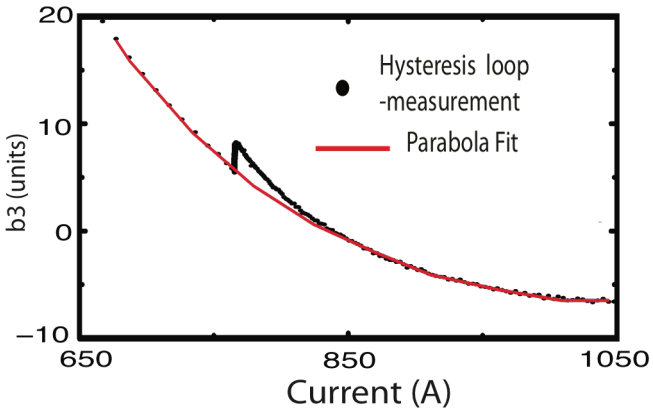

Fig. 5. An example of long snapback observed in MBH magnets at injection current of 760 A.

describes statistically well this branch of the curve (Fig. 5). After the parameterization, we correct the snapback curve subtracting the fitted parabola from the measurement points.

In this analysis, we describe the snapback time dependence by a half Gaussian, where t = 0 is at the beginning of the current ramp:

$$\Delta b_3^{sb}(t) = \Delta b_3^{dec}(t_{inj}^{end}) \cdot \exp\left(\frac{-t^2}{t_{sb}^2}\right). \quad (3)$$

We found that Eq. 3 statistically fits the snapback in case of the Tevatron dipoles. Equation 3 is equivalent to LHC description of the decay (see [14], Eq. 3) with the assumption of a parabolic increase of the current with time, $\Delta I = a\ t_{sb}^2$, after the injection. This type of ramp is normally used at the LHC operations.

Figure 5 shows a typical decay for MBHDP01 magnets at 760 A. After removing the underlying hysteresis loop, marked with continuous line, we see a long snapback that spans from 760 to 840 A. This length of snapback is untypical for NbTi magnets. A similar result was shown in [4] for one of the CERN 11 T Nb_3Sn dipole.

To perform a better comparison between the snapbacks from different magnets, we plot the change of the normal sextupole (Δb_3^{sb}) versus the time. Figure 6 shows Δb_3^{sb} for the MBH dipoles at 760 A. The beginning of the snapback, t = 0, is defined when the current starts parabolically to increase for

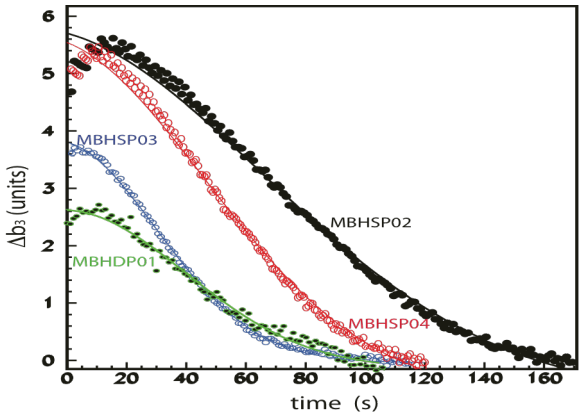

Fig. 6. Snapback in MBH magnets at 760 A. The snapback duration is significantly longer compared to NbTi magnets.

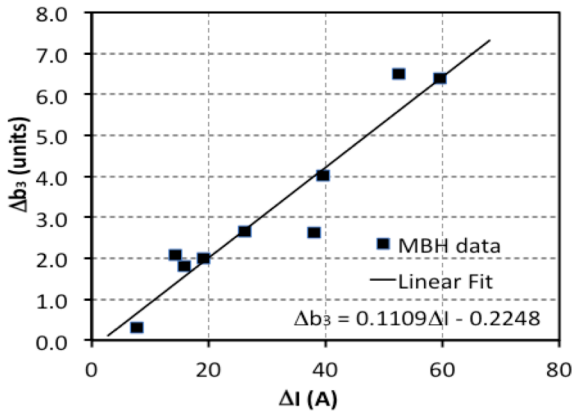

Fig. 7. Decay/Snapback Δb_3 amplitude versus ΔI the in the analyzed MBH magnets.

beam acceleration. The lines in Fig. 6 represent the half Gaussian fit with Eq. 3. In comparison to NbTi magnets, we observe significant increase of the snapback time, up to 10 times, while the decay amplitude is increasing only 3-4 times. Moreover, we observe an unexpected fast increase of the decay/snapback amplitude in the first 10-20 seconds of the current ramp. This phenomenon was found for the first time in these dipoles, which apparently may stem from fast dynamic effects, for example from Inter-Strand Coupling Currents [14].

To remove the dependence of the ramping rate, we present the decay/snapback amplitude as function of the current change ΔI at the beginning of the current ramp after injection. For the NbTi LHC and Tevatron production dipoles, empirically it was found [5, 9] that

$$\Delta b_3^{sb}(0) = \Delta b_3^{dec}(t_{inj}^{end}) \propto \Delta I. \quad (4)$$

This "scaling law" was employed in the mathematical formulation proposed to predict the harmonics of LHC magnets [14]. Figure 7 shows the linear fit to the $\Delta b_3^{sb}(0)$ dependence on ΔI for the data sets described in Table 1. The cycles with injection current of 350 A are excluded due to the large noise as discussed above. The fit returns an intercept close to zero (-0.22 units) and a slope of 0.11 units/A. The slope value is 50% smaller compared to the measured one in the Tevatron NbTi dipoles [5, 6], and is consistent with the larger decay amplitude and longer snapback time for MBH dipoles.

V. Conclusion

We presented a summary of the dynamic effects, including decay and snapback, in the main dipole and sextupole fields, for the 11 T Fermilab single-aperture models MBHSP02-04 and double-aperture model MBHDP01. The results clearly show that decay and snapback follow the same trend as NbTi dipoles. The main difference observed is in the amplitude of the decay in the normal sextupole, which was found to be on average 5.5 units at injection current of 760 A, a current dwell that is below the full penetration of the superconducting filaments. For comparison, the LHC and Tevatron NbTi dipoles, with injection currents above the full penetration of the superconducting filaments, had decay amplitude on the level of 1-2 units.

As a rule, the larger decay amplitude is followed by longer snapback. Compared to the measured NbTi dipoles, we found snapback time constants up to 10 times longer. This converts to up to 80 A in ΔI, the current needed to return the b_3 to the hysteresis curve, which is an order of magnitude larger than currents observed in the CERN MBH dipole models [3]. Moreover, the CERN MBH models show inverse dependence on the decay. Such discrepancies cannot be explained by different Nb_3Sn cables or different production processes: CERN and Fermilab are using the same cable and practically the same production procedures.

To characterize the behavior of the Nb_3Sn magnets, new models are being introduced and discussed, see [3, 11]. These models are exploring the specific features of the Nb_3Sn HEP conductor, like a large penetration field and flux jumps at low field, which are typically observed NB_3Sn but not NbTi strands. To confirm these models, more data from dedicated experiments are needed.

VI. Acknowledgment

The authors wish to thank the staff of Fermilab Technical Division for providing continuous support of these magnetic measurements over the course of the past years.

References

[1] D. A. Finley, *et al.*, "Time Dependent Chromaticity Changes in the Tevatron*", Proc. 1987 PAC*, Washington, DC, 1987, pp. 151-153.
[2] M. Haverkamp, "Decay and Snapback in Superconducting Accelerator Magnets", PhD Thesis, University of Twente, Netherlands, 2003.
[3] S. Izquierdo Bermudez, L. Bottura, L. Fiscarelli, E. Todesco, "Decay and Snapback in Nb_3Sn Dipole Magnets", *IEEE Trans. Appl. Supercond.,* vol. 27, no. 4, 2017, Art. 4002306.
[4] R. W. Hanft, *et al*., "Studies of Time Dependent fields in Tevatron Superconducting Dipole Magnets", IEEE Trans. Moan, 25, No. 2, 1989.
[5] G. Annala, *et al*., "Measurements of Geometric, Hysteretic and Dynamic Sextupole in Tevatron Dipoles", Fermilab note TD-04-043. [Online]. Available at: http://www-tdserver1.fnal.gov/project/TDlibry/TD-Notes/2004%20tech%20Notes/TD-04-043.pdf
[6] G. Velev, *et al.*, "Measurements of the Persistent Current Decay and Snapback Effect in Tevatron Dipole Magnets", *IEEE Trans. Appl. Supercond.*, vol. 17, no. 2, 2007, pp. 1105-1108.
[7] H. Brück, *et al.,* "Time Dependence of Persistent Current Effects in the Superconducting HERA Magnets", Contribution to the 11th International Conference on Magnet Technology - MT-11, Tsukuba, Japan, Aug. 28-Sep. 1, 1989.
[8] W. Fisher, A. Jain and S.Tepikian, "Beam-based measurements of the persistent current decay in RHIC", *Phys. Rev. Spec. Top. Accel. Beams*, vol. 4, 2001, 041002.
[9] L. Bottura, T. Pieloni, S. Sanfilippo, G. Ambrosio, P. Bauer and M. Haverkamp, Proceedings of European Accelerator Conference, Lucerne, Switzerland, 2004, pp. 1609–1611.
[10] A. V. Zlobin, *et al.*, "Development of Nb_3Sn 11 T Single Aperture Demonstrator Dipole for LHC Upgrades", *Proc. 2011 PAC*, New York, pp. 1460-1462.
[11] G. Velev, *et al*., "Summary of the Persistent Current Effect Measurements in Nb_3Sn and NbTi Accelerator Magnets at Fermilab", *IEEE* Trans. *Appl. Supercond*., Vol. 26, No. 4, 2016, Art. 4000605.
[12] J. DiMarco, *et al.,* "Application of PCB and FDM Technologies to Magnetic Measurement Probe System Development", *IEEE* Trans. *Appl. Supercond*., Vol. 23, No. 3, 2013, Art. 9000505.

[13] G.V. Velev, *et al.,* "A fast continuous magnetic field measurement system based on digital signal processors", *IEEE* Trans. *Appl. Supercond*., Vol. 16, No. 2, 2006, pp. 1374-1377.
[14] N. J. Sammut, *et al*., "Mathematical formulation to predict the harmonics of the superconducting Large Hadron Collider magnets", *Phys. Rev. ST Accel. Beams* 10, 082802, 2007.